

1 **A betacoronavirus multiplex microsphere immunoassay detects early SARS-CoV-2**
2 **seroconversion and controls for pre-existing seasonal human coronavirus antibody**
3 **cross-reactivity**
4

5 Eric D. Laing^{1*}, Spencer L. Sterling^{1,3}, Stephanie A. Richard^{2,3}, Shreshta Phogat^{1,3}, Emily C.
6 Samuels^{1,3}, Nusrat J. Epsi^{2,3}, Lianying Yan^{1,3}, Nicole Moreno^{2,3}, Christian Coles^{2,3}, Jennifer
7 Mehalko⁴, Matthew Drew⁴, Caroline English^{2,3}, Kevin K. Chung⁵, G. Travis Clifton⁶, Vincent J.
8 Munster⁷, Emmie de Wit⁷, David Tribble², Brian K. Agan^{2,3}, Dominic Esposito⁴, Charlotte
9 Lanteri², Edward Mitre¹, Timothy H. Burgess², and Christopher C. Broder^{1*}

10
11

12

13 ¹Department of Microbiology and Immunology, Uniformed Services University of the Health
14 Sciences, Bethesda, MD, USA

15 ²Infectious Diseases Clinical Research Program, Department of Preventive Medicine and
16 Biostatistics, Uniformed Services University of the Health Sciences, Bethesda, MD, USA

17 ³Henry M. Jackson Foundation for the Advancement of Military Medicine, Inc., Bethesda, MD
18 USA

19 ⁴Protein Expression Laboratory, National Cancer Institute RAS Initiative, Frederick National
20 Laboratory for Cancer Research, Frederick, MD, USA

21 ⁵Department of Medicine, Uniformed Services University of the Health Sciences, Bethesda, MD,
22 USA

23 ⁶Brooke Army Medical Center, JBSA Fort Sam Houston, TX, USA

24 ⁷Laboratory of Virology, Rocky Mountain Laboratories, National Institute of Allergy and
25 Infectious Diseases, National Institutes of Health, Hamilton, MT, USA

26

27

28 *Correspondence

29 Eric D. Laing, PhD

30 Department of Microbiology and Immunology

31 Uniformed Services University, Bethesda, MD 20814

32 Phone: 301-295-9884

33 Fax: 301-295-1545

34 Email: eric.laing@usuhs.edu

35 Christopher C. Broder, PhD

36 Department of Microbiology and Immunology

37 Uniformed Services University, Bethesda, MD 20814

38 Phone: 301-295-3401

39 Fax: 301-295-1545

40 Email: christopher.broder@usuhs.edu

41

42 **ABSTRACT**

43 With growing concern of persistent or multiple waves of SARS-CoV-2 in the United States,
44 sensitive and specific SARS-CoV-2 antibody assays remain critical for community and hospital-
45 based SARS-CoV-2 surveillance. Here, we describe the development and application of a
46 multiplex microsphere-based immunoassay (MMIA) for COVID-19 antibody studies, utilizing
47 serum samples from non-human primate SARS-CoV-2 infection models, an archived human
48 sera bank and subjects enrolled at five U.S. military hospitals. The MMIA incorporates prefusion
49 stabilized spike glycoprotein trimers of SARS-CoV-2, SARS-CoV-1, MERS-CoV, and the
50 seasonal human coronaviruses HCoV-HKU1 and HCoV-OC43, into a multiplexing system that
51 enables simultaneous measurement of off-target pre-existing cross-reactive antibodies. We
52 report the sensitivity and specificity performances for this assay strategy at 98% sensitivity and
53 100% specificity for subject samples collected as early as 10 days after the onset of symptoms.
54 In archival sera collected prior to 2019 and serum samples from subjects PCR negative for
55 SARS-CoV-2, we detected seroprevalence of 72% and 98% for HCoV-HKU1 and HCoV-OC43,
56 respectively. Requiring only 1.25 μ L of sera, this approach permitted the simultaneous
57 identification of SARS-CoV-2 seroconversion and polyclonal SARS-CoV-2 IgG antibody
58 responses to SARS-CoV-1 and MERS-CoV, further demonstrating the presence of conserved
59 epitopes in the spike glycoprotein of zoonotic betacoronaviruses. Application of this serology
60 assay in observational studies with serum samples collected from subjects before and after
61 SARS-CoV-2 infection will permit an investigation of the influences of HCoV-induced antibodies
62 on COVID-19 clinical outcomes.

63

64

65

66 INTRODUCTION

67 Severe acute respiratory syndrome coronavirus-2 (SARS-CoV-2) is a novel zoonotic
68 positive-sense, single-stranded, RNA virus responsible for the third viral pandemic of the 21st
69 century, and the third zoonotic coronavirus outbreak in the past 20 years (1, 2). At this time,
70 SARS-CoV-2 has globally caused 34 million COVID-19 cases and over 1 million COVID-19
71 related deaths. A major concern of the ongoing SARS-CoV-2 pandemic has been the frequent
72 reports of waning virus-specific antibody levels, with several studies reporting decay to
73 undetectable levels within just a few months after infection (3-5). While this is a measurable
74 feature of antibody response, it is also possible that current assays lack the sensitivity required
75 to detect lower levels of SARS-CoV-2 specific antibodies. To date, a variety of antibody tests
76 have been developed with 38 tests granted Emergency Use Authorization (EUA) by the U.S.
77 Food and Drug Administration. The majority of these tests assess for antibodies against the
78 coronavirus spike (S) envelope glycoprotein, the primary target of virus-neutralizing antibodies
79 (6), in either its native-like oligomer conformation, or against one of its protein subunits or
80 domains. In general, most S glycoprotein antigen-based assays report the ability to detect
81 antibodies in 65-70% of infected individuals 8 – 14 days after symptom onset, with positivity
82 rates over 90% not occurring until 2 – 3 weeks after symptom onset (7).

83 In this study, we describe the development, characterization, and utility of a
84 betacoronavirus (β -CoV) multiplex microsphere-based immunoassay (MMIA) for COVID-19
85 serology studies. To optimize sensitivity and specificity for measuring SARS-CoV-2 spike
86 reactive antibodies, the MMIA included prefusion stabilized S glycoprotein ectodomain trimers of
87 SARS-CoV-2, SARS-CoV-1, MERS-CoV, and the seasonal human coronaviruses (HCoV),
88 HCoV-HKU1 and HCoV-OC43. The MMIA enabled the simultaneous measurement of relative
89 antibody quantities against each of these medically-relevant betacoronaviruses. We
90 hypothesized that this approach would potentially result in a highly sensitive and specific assay

91 for detecting SARS-CoV-2 specific antibodies through two mechanisms. First, the Luminex
92 xMAP-based platform has a large dynamic range and has been shown to be more sensitive
93 than ELISA for the detection of antibodies to other viral infections (8-10). Second, given the high
94 seroprevalence of the common human betacoronaviruses (11-13), cross-reactive antibodies
95 present in subject samples (14, 15) could be concurrently measured and accounted for in a
96 multiplex approach. By testing for S glycoprotein reactive antibodies to SARS-CoV-2 in the
97 presence of HKU1 and OC43 S glycoproteins, the MMIA assay controls for off-target pre-
98 existing cross-reactive betacoronavirus antibodies, thus enhancing specific SARS-CoV-2
99 antibody detection. Additionally, the simultaneous incubation of serum with S glycoproteins from
100 all the relevant betacoronaviruses may enable a lower threshold for SARS-CoV-2 antibody
101 positivity.

102 Utilizing serum samples from an experimentally challenged non-human primate (NHP)
103 model, together with human sera from subjects confirmed to have SARS-CoV-2 infection and
104 from subjects confirmed to have other coronavirus infections collected prior to 2018, we report
105 the sensitivity and specificity performances for this assay strategy. Serum samples from rhesus
106 macaques experimentally infected with SARS-CoV-2 demonstrated that SARS-CoV-2 S
107 glycoprotein IgG seroconversion was detectable by 10 days post infection (dpi), consistent with
108 other reports demonstrating anti-S glycoprotein IgG seroconversion between 3 and 14 dpi (16-
109 19). As a result, we evaluated serum samples from SARS-CoV-2 positive subjects collected 10
110 days after symptom onset and report 98% sensitivity for SARS-CoV-2 S glycoprotein IgG
111 antibody detection in humans at that time point. We also examined differences in SARS-CoV-2
112 antibody reactivity between widely used antigens: SARS-CoV-2 prefusion stabilized S
113 glycoprotein ectodomain trimer and the receptor-binding domain (RBD). High seroprevalence of
114 seasonal HCoV OC43 and HKU1, ranging from 97 – 98% and 55 – 89%, respectively, was
115 observed across both archival sera and SARS-CoV-2 negative subject serum samples. Through

116 this MMIA strategy we aim to investigate the interplay of pre-existing seasonal HCoV antibodies
117 on SARS-CoV-2 IgG duration, COVID-19 symptom presentation, and disease severity.
118 Preliminary data we have obtained using this multiplex serology strategy demonstrates that
119 SARS-CoV-2 antibody can be detected early after the onset of symptoms and that
120 SARS-CoV-2 infection can stimulate an IgG antibody response that is cross-reactive with
121 SARS-CoV-1 and MERS-CoV S glycoproteins.

122

123 **RESULTS**

124 *Comparison of MMIA and ELISA for SARS-CoV-2 IgG antibody detection*

125 We first established our ability to detect SARS-CoV-2 IgG and monitor SARS-CoV-2
126 seroconversion with sera collected from SARS-CoV-2 infected NHP. Purified IgG from SARS-
127 CoV-2 infected NHP collected 21 dpi were pooled and spiked into NHP negative sera, and the
128 MMIA was quantitatively characterized for IgG polyclonal reactivity revealing SARS-CoV-2 spike
129 antibody MFI curve linearity between 0.625 – 5.0 µg/ml or 3690 – 20,354 MFI (Figure 1).
130 Positive MMIA saturation occurs within 20,000 – 30,000 MFI. To investigate the effects of the
131 increased dynamic range facilitated by Luminex xMAP-based multiplexing systems on MMIA
132 sensitivity, we compared end-point titers by both ELISA and MMIA. In an ELISA, SARS-CoV-2
133 positive NHP sera end-point titers ranged from 1,000 to 2,000 (Figure 2A), consistent with
134 reported ELISA titers for these animals (16). In the MMIA, the ability to detect serially diluted
135 IgG antibodies was 4- to 8-fold greater than ELISA with end-point titers ranging from 4,000 (n=
136 2) to 16,000 (n= 1) (Figure 2B).

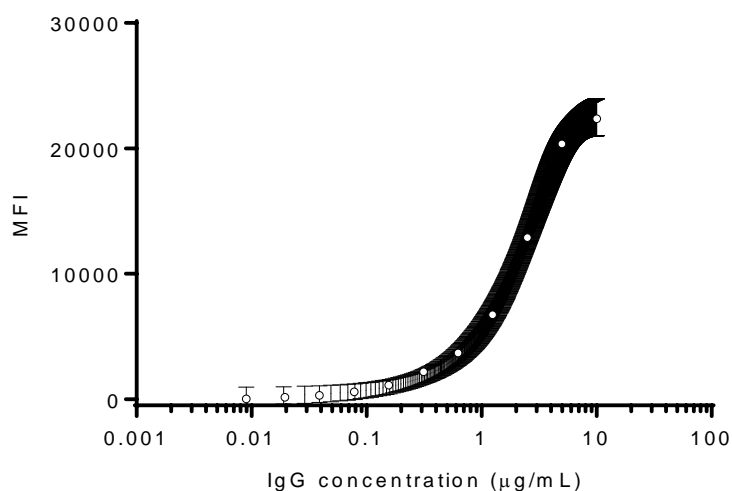
137

138

139

140

141



142

143

144 **Figure 1: SARS-CoV-2 spike protein reactivity as a function of IgG concentration. A**

145 sigmoidal curve was used to fit the MEAN±SEM of two independent experiments performed in

146 technical triplicates. MFI, median fluorescence intensities.

147

148

149

150

151

152

153

154

155

156

157

158

159

160
161
162
163
164
165
166
167
168
169
170
171
172
173
174
175
176
177
178
179
180
181
182
183
184
185

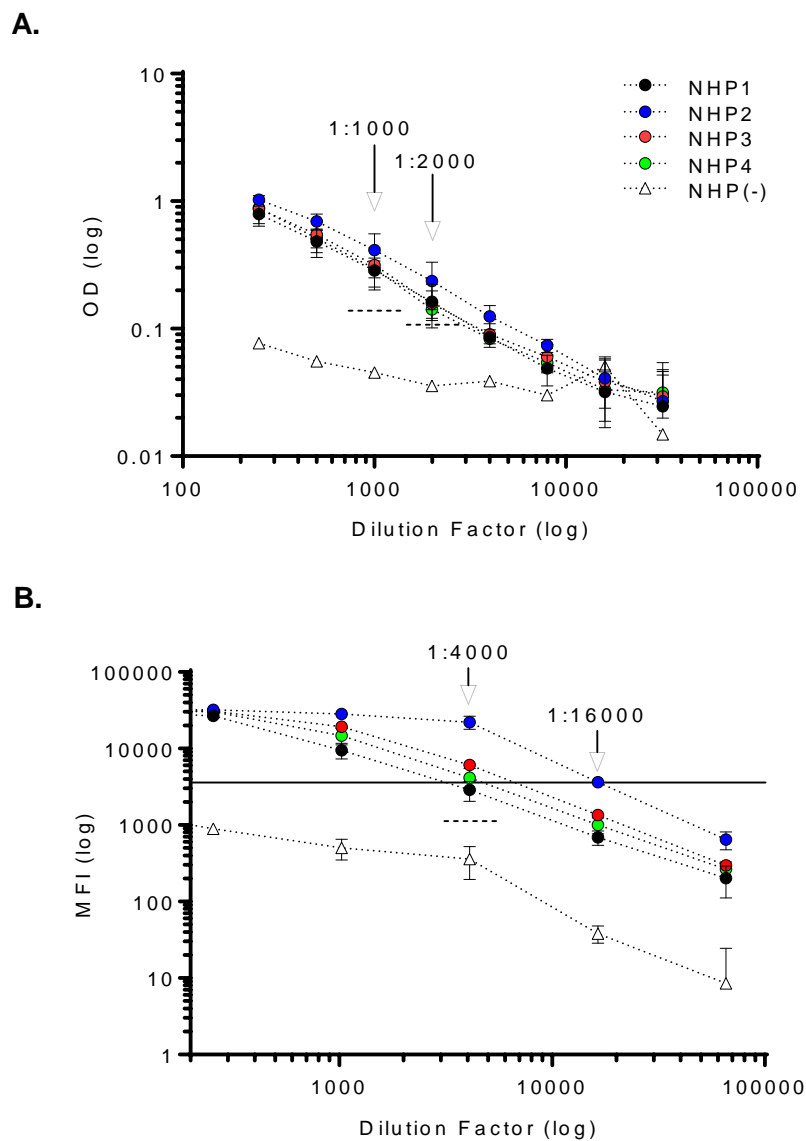


Figure 2. MMIA displays enhanced sensitivity for SARS-CoV-2 IgG detection. Serum samples from SARS-CoV-2 infected NHP collected 21 dpi were tested by SARS-CoV-2 spike protein **(A)** ELISA and **(B)** MMIA. **(A)** Dashed lines indicate 3-fold MFI above the NHP(-) serum sample(s) diluted 1:1000 and 1:2000. **(B)** A solid line indicates the lower limit of MFI linearity and a dashed line indicates 3-fold MFI above the NHP(-) serum sample diluted 1:4000. Positive samples are those above both the MFI level for curve linearity and 3-fold change in NHP(-) serum. MFI values represent MEAN \pm SD of two independent experiments performed in technical triplicates.

186 *Seroconversion in a non-human primate model*

187 Next, we monitored SARS-CoV-2 seroconversion with longitudinal NHP serum samples.
188 SARS-CoV-2 spike protein reactive IgG antibody seroconversion was observed in all four NHP
189 10 dpi (Figure 3A). We also investigated SARS-CoV-2 IgM antibody seroconversion and
190 detected IgM level above baseline in two NHP by 7 dpi; all four NHP had detectable IgM by 10
191 dpi (Figure 3B). Notably, IgG antibody from SARS-CoV-2 challenged NHP did not significantly
192 react with spike proteins from betacoronaviruses, SARS-CoV-1, MERS-CoV or HCoVs, included
193 in the MMIA (Figure 3A), whereas, a varying degree of IgM cross-reactivity was observed
194 (Figure 3B). Additionally, high baseline IgM reactivity to SARS-CoV-2 RBD at 0 dpi inhibited our
195 ability to ascertain the dpi where seroconversion could be observed with this SARS-CoV-2
196 antigen (Figure 3B).

197

198

199

200

201

202

203

204

205

206

207

208

209

210

211

212
213
214
215
216
217
218
219
220
221
222
223
224
225
226
227
228
229
230
231
232
233
234
235
236
237

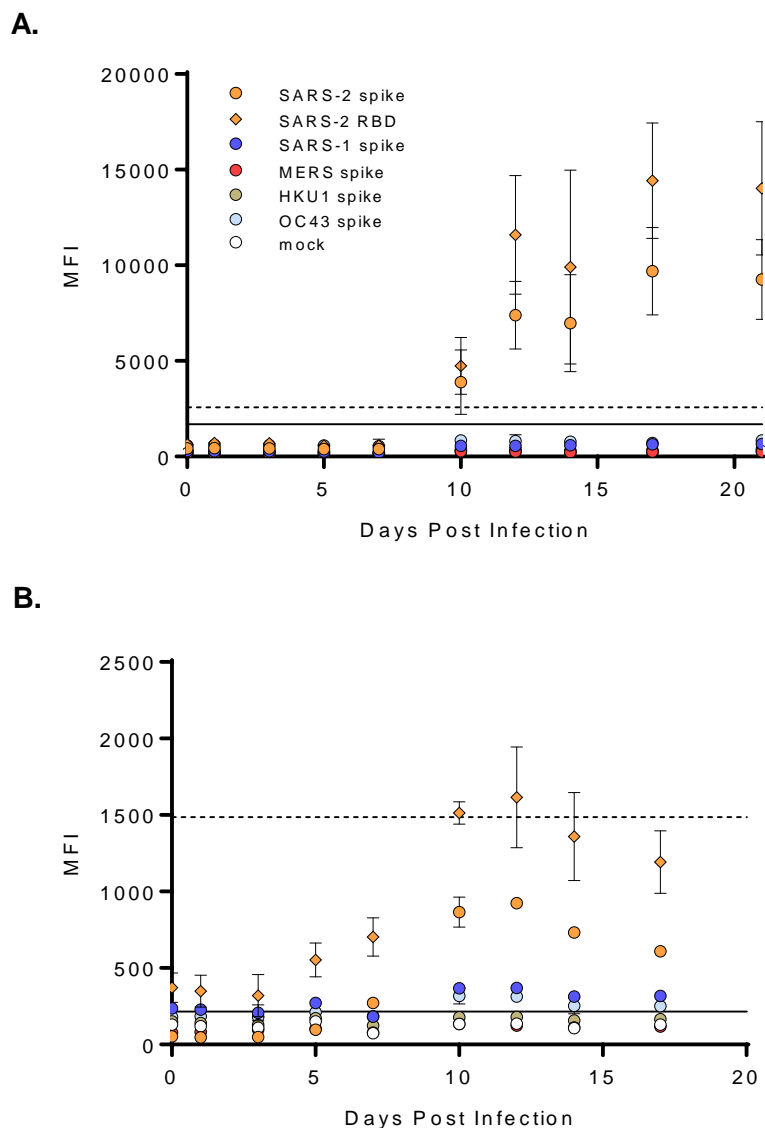


Figure 3. SARS-CoV-2 seroconversion in a non-human primate model. Sera from SARS-CoV-2 infected NHP were screened for SARS-CoV-2 spike protein reactive (A) IgG and (B) IgM. Graphs represent the MEAN \pm SD of four SARS-CoV-2 challenged NHP screened in two independent experiments performed in technical duplicates. A solid line indicates a 4-fold rise in SARS-CoV-2 spike protein MFI from baseline (0 dpi) and was used as a threshold cutoff for SARS-CoV-2 IgG and IgM seroconversion; a dashed line indicates a 4-fold rise in SARS-CoV-2 RBD protein MFI from baseline.

238 *Archival sera from subjects with PCR-confirmed seasonal coronaviruses exhibit cross-reactivity*
239 *with SARS-CoV-2 spike protein*

240 Despite low sequence similarity and identity between SARS-CoV-2 spike protein and
241 seasonal HCoV spike proteins, antibody cross-reactivity with SARS-CoV-2 proteins has been
242 observed (14, 15). To determine whether prior infection with seasonal HCoV induces antibodies
243 that cross-react with SARS-CoV-2, we assayed archival (pre-2019) serum from human subjects
244 with PCR-confirmed seasonal HCoVs. When setting a cut-off for positivity at three times the
245 mean MFI obtained for a mock antigen preparation-coupled microsphere, we observed that
246 8.89% (4/45) of archived serum samples from HCoV PCR-positive subjects cross-reacted with
247 SARS-CoV-2 spike protein (Figure 4A-D). Cross-reactivity between HCoV-induced antibodies
248 with SARS-CoV-2 spike protein was observed in subjects that were PCR-positive for OC43
249 (1/16), HKU1 (1/6) and 229E (2/10) infection.

250

251

252

253

254

255

256

257

258

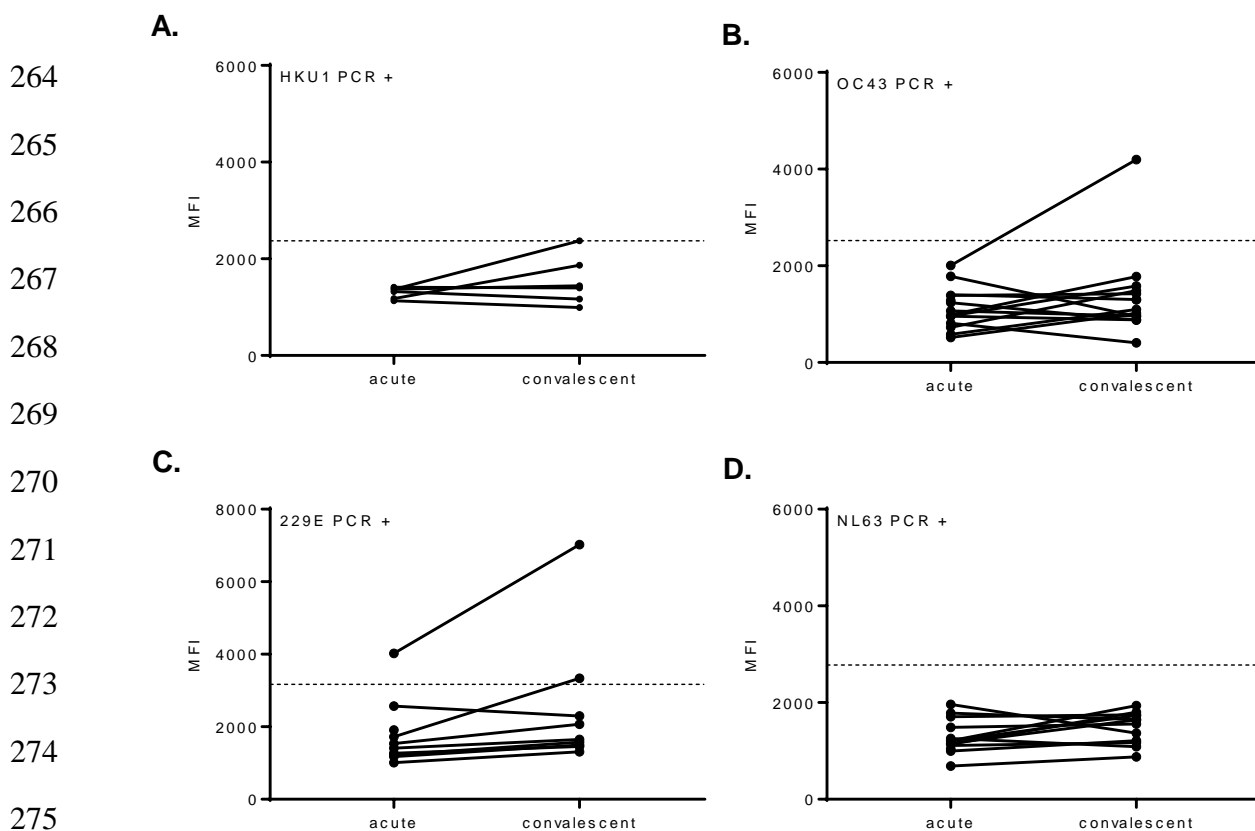
259

260

261

262

263



264
265
266
267
268
269
270
271
272
273
274
275
276
277 **Figure 4. Archival sera from subjects with seasonal HCoVs can display cross-reactivity**
278 **with SARS-CoV-2 spike protein.** Acute and convalescent serum samples from HCoV PCR-
279 positive subjects were tested in a β -CoV MMIA. Subjects are grouped together based on HCoV
280 PCR confirmation, **(A)** OC43 (n= 16), **(B)** HKU1 (n= 6), **(C)** NL63 (n= 13) and **(D)** 229E (n= 10),
281 A dashed line indicates the 3-fold change in the mean MFI of a mock antigen-coupled
282 microsphere. MFI values represent the MEAN of two independent experiments performed in
283 technical duplicates. MFI, median fluorescence intensity.

284
285
286
287
288
289

290 *Assay threshold cutoffs for SARS-CoV-2 spike protein reactive antibodies*

291 To control for pre-existing HKU1 and OC43 spike protein reactive antibody cross-
292 reactivity with SARS-CoV-2 spike protein, rather than using a cutoff of three times the mean MFI
293 obtained for mock antigen, antibody threshold cutoffs were established with HCoV PCR-positive
294 convalescent sera (Figure 5A-B). A conventional 99.7% probability, mean and three standard
295 deviations higher, threshold cutoff was employed to distinguish positive and negative IgG
296 antibodies. The mean IgG reactivity to SARS-CoV-2 spike protein was 1569 MFI with a 99.7%
297 probability threshold cutoff of 4911 MFI. The SARS-CoV-2 RBD protein had a notably higher
298 background IgG antibody reactivity and threshold cutoff, 2846 MFI and 7951 MFI, respectively.
299 Given the inherently less-specific nature of IgM, a 99.9% probability threshold cutoff was
300 preferred. The 99.9% probability threshold cutoffs for SARS-CoV-2 spike protein and RBD
301 protein reactive IgM were 846 MFI and 15352 MFI. The remaining archival sera (n= 84),
302 representing HCoV PCR-positive acute sera, rhinovirus PCR-positive acute/convalescent sera,
303 and acute/convalescent sera from 'no pathogen detected' subjects, did not react with SARS-
304 CoV-2 spike protein or RBD protein above the established threshold cutoffs for either antigen
305 (Figure 5C-D). Although only 17%/7% of ARIC human subjects were OC43/HKU1 PCR positive,
306 we observed 97.6% OC43 and 89.2% HKU1 IgG, and none were IgM positive (Figure 5C-D).
307 Interestingly, the three OC43 spike IgM positive serum samples were collected from subjects
308 who had no pathogen detected by PCR.

309

310

311

312

313

314

315

316

317

318

319

320

321

322

323

324

325

326

327

328

329

330

331

332

333

334

335

336

337

338

339

340

341

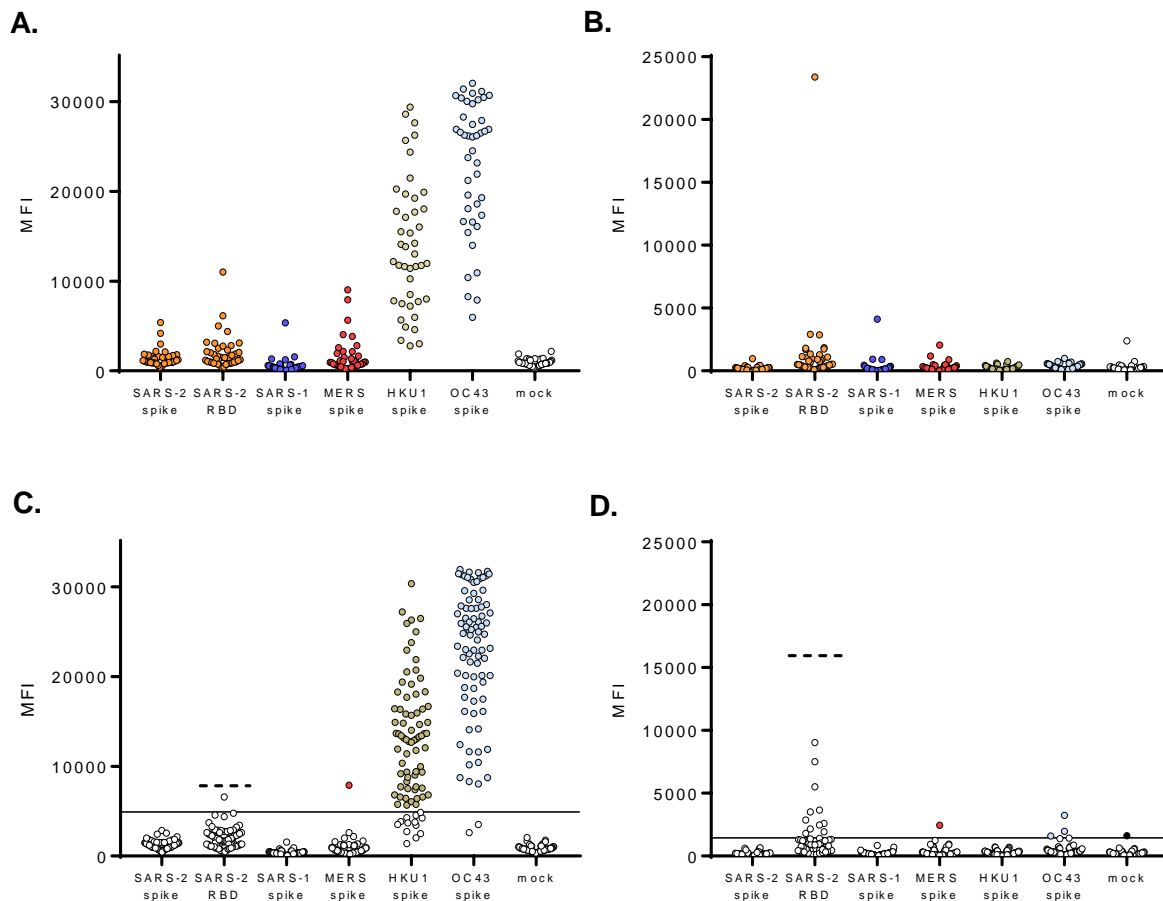


Figure 5. Archival sera generated threshold cutoffs for IgG and IgM antibodies confer

specificity for SARS-CoV-2. Convalescent serum samples (n= 43) from HCoV PCR-positive

subjects were tested in the β -CoV MMIA with **(A)** IgG antibody and **(B)** IgM antibody. **(C-D)**

Archival sera (n= 84), acute serum samples from HCoV PCR-positive subjects,

acute/convalescent serum samples from rhinovirus PCR-positive subjects and

acute/convalescent serum samples from 'no pathogen detected' subjects were tested for **(C)**

IgG and **(D)** IgM antibody reactivity tested against the established threshold cutoffs. A solid line

indicates the threshold cutoff for positivity with SARS-CoV-2 spike protein and a dashed line

indicates the threshold cutoff for SARS-CoV-2 RBD. Colored dots in **(C-D)** indicate samples with

MFI above the SARS-CoV-2 spike protein threshold cutoff for positive antibody. MFI is the

average of sera diluted 1:400, adjusted with PBS controls and tested across technical duplicate

plates. IgG data is a representation of three independent screenings.

342 *Multiplex microsphere-based immunoassay performance*

343 Sera from persons with SARS-CoV-2 infection were screened for IgG and IgM antibody
344 reactivity with betacoronavirus spike proteins in our MMIA. As SARS-CoV-2 seroconversion was
345 detected by 10 dpi in NHPs, MMIA SARS-CoV-2 spike protein IgG sensitivity for human
346 serology was evaluated in confirmed subjects \geq 10 days post-symptom onset (dpso).
347 Additionally, a combination of archival human serum samples, and PCR negative MTF
348 hospitalized subjects and outpatients with serum samples collected < 30 dpso were included in
349 a negative agreement analysis. Subjects that were PCR confirmed as SARS-CoV-2 negative
350 displayed no IgG with SARS-CoV-2 spike protein, whereas one subject had IgM reactivity to
351 SARS-CoV-2 spike protein above the 99.9% cutoff MFI value. A receiver operating
352 characteristic (ROC) curve analysis was then performed to further establish a more
353 conservative threshold value (1446 MFI cutoff point) for SARS-CoV-2 positive IgM (Figure 6A-
354 B). Further, HKU1 and OC43 IgG antibodies were observed in SARS-CoV-2 PCR negative
355 subjects (Figure 6A). SARS-CoV-2 reactive IgG antibodies were only detected above the 99.7%
356 threshold cutoff in the PCR positive subjects enrolled at military hospitals or the Javits Center
357 field hospital; cross-reactive antibodies to SARS-CoV-1 and MERS-CoV were observed in
358 SARS-CoV-2 PCR positive and IgG positive subjects (Figure 6B).

359

360

361

362

363

364

365

366

367

368

A.

369

370

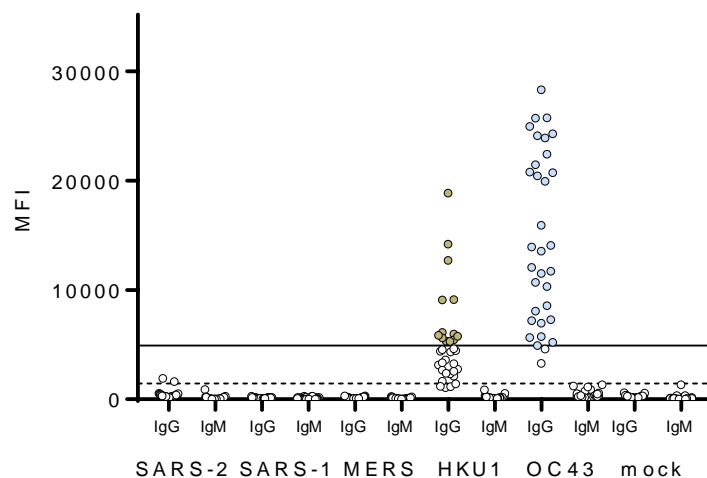
371

372

373

374

375



376

B.

377

378

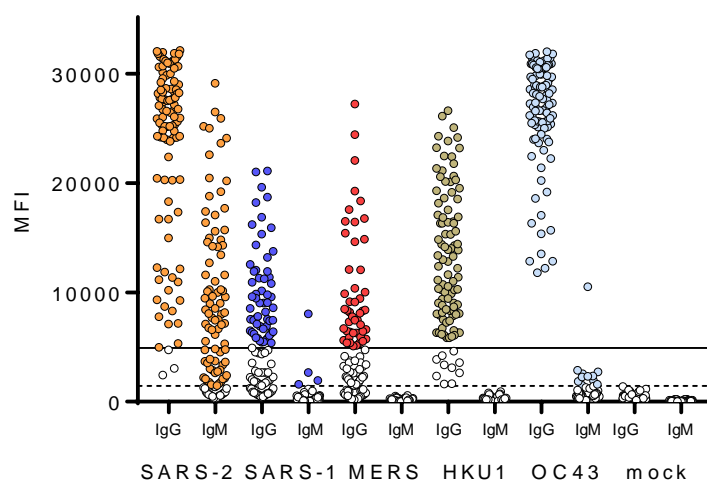
379

380

381

382

383



384

385

386 **Figure 6. A multiplex antibody test can detect SARS-CoV-2 specific and cross-reactive**

387 **antibodies.** Serum samples from **(A)** SARS-CoV-2 PCR negative subjects **(B)** SARS-CoV-2

388 PCR-positive subjects collected ≥ 10 dpso were tested by β -CoV MMIA. Serum were diluted

389 1:400 and tested in duplicate plates. MFI, median fluorescence intensities, are the average of

390 PBS-subtracted technical duplicates. A solid line indicates the IgG threshold cutoff and a

391 dashed line indicates the IgM threshold cutoff. Colored dots indicate positive serum samples.

392 SARS-2, SARS-COV-2; SARS-1, SARS-CoV-1; MERS, MERS-CoV; HKU1, HCoV-HKU1;

393 OC43, HCoV-OC43.

394 Performance assessments of this β -CoV MMIA for SARS-CoV-2 spike protein IgG and
395 IgM detection are included in Table 1. SARS-CoV-2 spike protein reactive IgG antibody
396 detection was calculated with 95% confidence intervals (CI) as follows, sensitivity = 98.06%
397 (94.45% – 99.60% CI), specificity= 100% (96.82% – 100.00% CI). Assuming a US disease
398 prevalence of 1.0%, the positive predictive value (PPV) = 100.00%, and negative predictive
399 value (NPV) = 99.98% (99.94% - 99.99% CI). SARS-CoV-2 spike protein reactive IgM detection
400 sensitivity was lower than IgG, with performance analysis conducted with serum samples
401 collected \geq 7 days post-symptom onset, sensitivity= 78.10% (68.97% to 85.58%), specificity=
402 100% (96.95% - 100.00% CI) and PPV= 100.00% (Table 1).

403 When comparing spike protein and RBD, notably, utility of SARS-CoV-2 RBD for IgG
404 detection had a reduced sensitivity (87.10%, 80.78% - 91.94% CI) (Table 2). To assess MMIA
405 precision, three positive and one negative samples were tested over five independent
406 experiments, with at least two distinct in-house antigen-coupled bead lots and serum sample
407 freeze-thaws. Coefficient of variations (CV) were calculated for all three positive samples and
408 remained $<$ 20% (Figure 7). Although the negative sample had a $>$ 20%, the MFI never went
409 above the threshold cutoff for positive IgG across five independent tests.

410

411

412

413

414

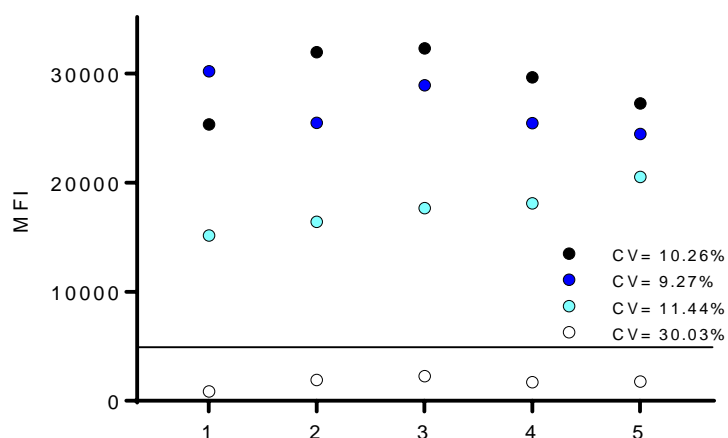
415

416

417

418

419



420

421 **Figure 7. Positive and negative results are reproducible over independent MMIA tests.**

422 Selected positive(s) and negative serum samples were tested across independent experiments.

423 CV, coefficient of variation, percentages are indicated on the graphs for each sample. A solid

424 line indicates the threshold cutoff for positive IgG.

425

426

427

428

429

430

431

432

433

434

435

436

437

438

439 **DISCUSSION**

440 In this study, we have demonstrated that use of a multiplex microsphere-based
441 immunoassay (MMIA) built using Luminex xMAP-based technology in which individual
442 microspheres are bound to pre-fusion stabilized S glycoprotein trimers of SARS-CoV-2, SARS-
443 CoV-1, MERS-CoV, and each of the two seasonal betacoronaviruses enables highly sensitive
444 and specific detection of SARS-CoV-2 IgG antibodies. In contrast to commercial ELISA and
445 lateral flow assays for SARS-CoV-2 IgG, which typically have a sensitivity in the range of 65-
446 70% up to 14 days after symptom onset (7), the MMIA has a sensitivity of 98% at just 10 days
447 after symptom onset in PCR-confirmed cases of SARS-CoV-2 infection. Use of this highly
448 sensitive assay will allow for improved assessments of the kinetics of humoral responses to
449 SARS-CoV-2 infection.

450 We hypothesize that the high sensitivity and specificity of the MMIA assay is due both to
451 the physics of the Luminex xMAP-based platform, which enables a high dynamic range of
452 measurement, as well as to the use of a multiplexing system. Multiplex microsphere-based
453 immunoassays have been shown to be more sensitive than standard ELISA for SARS-CoV-2
454 antibody detection (20) and several other virus infections, including Lassa virus, Ebola virus,
455 and simian immunodeficiency virus (8-10). Additionally, and perhaps more importantly,
456 simultaneously incubating serum against spike proteins of seasonal HCoVs may enable the
457 establishment of a lower threshold of positivity for detection of SARS-CoV-2 antibodies. Given
458 the presence of cross-reactive antibodies, assays that only test for antibodies against SARS-
459 CoV-2 may have to utilize a high signal threshold as a cut-off for positivity to reduce false
460 positive rates of detection. By incubating serum against multiple coronavirus spike proteins, the
461 MMIA platform may allow preferential binding of cross-reactive antibodies to the antigens of the
462 coronavirus against which they were initially induced, enabling a lower, and potentially more
463 sensitive, cut-off for the detection of SARS-CoV-2 specific antibodies.

464 Now nine months into the COVID-19 pandemic, this β -CoV MMIA adds to an established
465 body of antibody tests and serology results. Early in the pandemic, SARS-CoV-2 IgG
466 seroconversion was surprisingly detected early after exposure and sometimes in parallel with
467 IgM seroconversion (21-23). The temporal window to capture SARS-CoV-2 IgM is shorter than
468 IgG, and with IgG seroconversion occurring 10 dpi in NHP SARS-CoV-2 disease models, and
469 detectable as early as 7 dpso in subjects, there appears little benefit for continued SARS-CoV-2
470 IgM detection (Table 3). As we placed no upper limit on the dpso of the first serum collection
471 included in performance analysis, IgM sensitivity is lower than IgG driven by outpatient
472 enrollments in the EPICC, IDCRP-085 study on average 28 dpso that were IgG positive, but IgM
473 negative. Although less sensitive and less specific than IgG detection, the benefit of IgM
474 detection may lay in its ability to place a temporal window on SARS-CoV-2 exposure in
475 asymptomatic IgG positive individuals, particularly useful for cross-sectional studies of
476 seroprevalence.

477 Conservation of epitopes present in the prefusion stabilized native-like trimeric S
478 glycoprotein oligomers may be the major factor in the observed cross reactions between the
479 CoV S glycoproteins. Since the RBD protein is only a domain within the S1 subunit of the S
480 glycoprotein and lacks potentially conserved protein residues with seasonal HCoV S
481 glycoproteins, utility in antigen-based immunoassays confers specificity for SARS-CoV-2 and is
482 thus employed in several antibody tests (24-27). We noted that in the present β -CoV MMIA, the
483 commercially sourced RBD protein, which shares an equivalent number of protein residues with
484 the expressed RBD protein used in a microsphere-based immunoassay developed by the
485 Ragon Institute of MGH, MIT and Harvard (20), had a higher threshold cutoff that limited IgG
486 detection sensitivity compared to the spike protein. This reactivity to RBD may be driven by
487 artificial epitopes, exposure of epitopes otherwise inaccessible within the context of the native-
488 like S glycoprotein trimer or a product of microsphere coupling.

489 Immunoassay detection of IgG antibodies that can bind to RBD has been used as a
490 surrogate for neutralization tests which require cell-culture, pseudoviruses, or biosafety-
491 containment and wild-type SARS-CoV-2 (25, 28, 29). SARS-CoV-2 neutralizing antibodies
492 target the S glycoprotein S1 subunit, particularly the RBD and N-terminal domains, and
493 sterically interfere with human ACE-2 receptor interaction (30-34). Yet, SARS-CoV-2 and
494 MERS-CoV neutralizing monoclonal antibodies have been identified that binds epitopes that do
495 not interfere with receptor engagement (35, 36). Furthermore, non-neutralizing antibody-
496 mediated protection has been observed in other virus infections, including HIV and Ebola virus
497 (37, 38). Given the relatively poor performance of this RBD protein in this β -CoV MMIA, and our
498 ability to capture the full-breadth of the humoral response, e.g., RBD-binding, neutralizing and
499 non-neutralizing, to SARS-CoV-2 infection with the native-like spike protein trimer (39), future
500 studies will exclude the monomeric RBD antigen from β -CoV MMIA strategy.

501 The MMIA approach provided additional antibody detection data that is suggestive of
502 SARS-CoV-2 IgG cross-reactivity with SARS-CoV-1 and MERS-CoV. Conserved cross-
503 neutralizing epitopes between MERS-CoV, SARS-CoV-1 and SARS-CoV-2 S glycoproteins
504 have been identified (35, 40). Whether SARS-CoV-2 induced polyclonal IgG antibody responses
505 to SARS-CoV-1 and MERS-CoV spike proteins are retained after affinity maturation, or are
506 cross-neutralizing requires further investigation. Future studies with this MMIA will incorporate
507 spike proteins from the seasonal alphacoronaviruses, HCoV-NL63 and HCoV-229E, to improve
508 upon specificity for SARS-CoV-2 antibody detection. We hypothesize that the inclusion of NL63
509 and 229E spike proteins will provide additional off-target control of cross-reactive antibodies to
510 SARS-CoV-2 spike protein, decreasing the threshold cutoff for positive SARS-CoV-2 and
511 enabling improved detection of waning and low positive SARS-CoV-2 IgG antibody. To attempt
512 to achieve similar success at detecting SARS-CoV-2 antibodies and seroprevalence four
513 months after diagnosis (41), next steps in MMIA development will be focused on a re-calibration
514 of threshold cutoffs using archived sera in an MMIA that is limited to spike proteins from SARS-

515 CoV-2, HCoV-HKU1, HCoV-OC43, HCoV-NL63 and HCoV-229E. Importantly, when utilized in
516 select subject cohorts from prospective, longitudinal observational studies in which serum
517 samples are obtained before SARS-CoV-2 infection, this MMIA approach has the potential to
518 measure antibody cross reactions with seasonal HCoVs, and investigate whether HCoV-
519 induced antibodies confer any protection against COVID-19.

520

521 **CONCLUSION**

522 In summary, we have presented the development of a multiplex microsphere-based
523 immunoassay for SARS-CoV-2 serology that includes envelope spike glycoproteins from
524 zoonotic, SARS-CoV-1 and MERS-CoV, and seasonal endemic betacoronaviruses, HCoV-
525 HKU1 and HCoV-OC43. Performance assessment of this immunoassay with serum samples
526 from a pre-2019 archived sera bank and SARS-CoV-2 PCR positive subjects who sought
527 medical treatment at military hospitals demonstrated 100% specificity for SARS-CoV-2 IgG
528 antibody detection and 98% sensitivity with samples collected as early as 10 days after the
529 onset of symptoms. Through this multiplex approach we are able to measure the potential cross
530 reactions of HCoV-induced antibodies to SARS-CoV-2 spike glycoproteins. Application of this
531 multiplex approach to prospective observational studies will enable the direct examination of
532 whether pre-existing HCoV-induced antibodies affect COVID-19 clinical outcomes, i.e.
533 asymptomatic presentation and symptomatic severity.

534

535 **MATERIALS AND METHODS**

536 *Recombinant protein antigens and microsphere coupling*

537 Prefusion stabilized SARS-CoV-2 S-2P glycoprotein ectodomain trimers (hereafter
538 referred to as spike protein) and SARS-CoV-2 RBD were purchased from LakePharma, Inc.
539 (Hopkinton, MA USA). This SARS-CoV-2 spike protein shares an equivalent ectodomain with

540 the NIH Vaccine Research Center designed SARS-CoV-2 S-2P protein, and the Mount Sinai
541 SARS-CoV-2 S-2P protein used in ELISA-based serology (26, 27, 42-44). Differences between
542 LakePharna, Inc. and VRC or Mount Sinai spike protein constructs are highlighted in the C-
543 terminus tags and selection of mammalian cell-line for expression.

544 Design and expression of prefusion stabilized HCoV-HKU1, HCoV-OC43, SARS-CoV-1
545 and MERS-CoV spike proteins have been previously described (15, 42). A mock antigen,
546 consisting of cell culture supernatant from untransfected HEK cells was collected via
547 centrifugation then filtered through a 0.22 μ M PES filter to remove debris. Mock antigen-coupled
548 beads are included in each microtiter well to control for non-specific/artificial antisera binding;
549 samples that react with the mock antigen above an established 3-fold cutoff are retested. Spike
550 proteins were coupled to carboxylated magnetic MagPlex microspheres (Bio-Rad, Hercules,
551 CA) at a protein to microsphere ratio of 15 μ g:100 μ L, and antigen-coupled microspheres were
552 resuspended in a final volume of 650 μ L following manufacturer's protocol (Bio-Rad) for amine
553 coupling.

554 *Non-human primate sera*

555 Archived sera were used from rhesus macaques inoculated with a total dose of 2.6×10^6
556 TCID₅₀ of SARS-CoV-2 via a combination of intranasal, intratracheal, oral and ocular
557 inoculation routes (16). Serum samples were collected at dpi 0 (baseline), 1, 3, 5, 7, 10, 12, 14,
558 17 and 21. To purify serum IgG antibody, 250 μ L of serum from each of four experimentally
559 infected NHPs collected 21 dpi were pooled then subjected to thermal inactivation for 30 minutes
560 at 60 °C. During inactivation, 2 mL of Protein G agarose, 50% suspension (Sigma-Aldrich, St.
561 Louis, Missouri, USA) was added to a chromatography column and the buffer was allowed to
562 flow through. The bead bed was then washed three times with 10 mL of PBS. Inactivated
563 pooled sera were diluted 1:5 in PBS then added to the column. Flow-through was collected,
564 then re-added to the column; this process was repeated for a total of three passes through the

565 column. The bead bed was again washed three times with 10 mL of PBS. Finally, IgG was
566 eluted from the Protein G agarose using a 0.1M Glycine elution buffer, pH 2.5 then returned to
567 neutral pH using 1M Tris-HCl, pH 8.0. Eluted IgG was concentrated using an Amicon Ultra
568 Centrifugal Filter unit (Merck Millipore, Burlington, Massachusetts, USA), and the buffer was
569 exchanged to a 1X PBS buffer containing 25% glycerol.

570 SARS-CoV-2 IgG and IgM antibody seroconversion was determined as the first dpi
571 where a 4-fold increase in the median fluorescence intensity (MFI) was measured compared to
572 the baseline sera collection. Between the 1:250 and 1:1000 dilutions, some NHP IgG antibody
573 reactivities were no longer saturating the upper level of the MMIA. We chose further sera
574 screening at a 1:400 dilution, retaining the ability of the MMIA to detect positives at near MMIA
575 saturation, i.e. >20,000 MFI, while still within the linear region of detection.

576 *Participant enrollment and sera collection*

577 SARS-CoV-2 negative human serum specimens utilized were from archived sera
578 collected between 2012 – 2018 in the Infectious Disease Clinical Research Program (IDCRP)
579 Acute Respiratory Infection Consortium Natural History Study (ARIC, IDCRP-045) (45). ARIC
580 sera predate the COVID-19 pandemic and were collected from subjects who had
581 nasopharyngeal swabs tested by nucleic acid amplification methods for virus etiologies of acute
582 respiratory infections; samples collected from individuals with rhinovirus and the seasonal
583 human coronaviruses HCoV-OC43, -HKU1, -229E and -NL63 were used (46). In addition,
584 serum samples were collected since the emergence of SARS-CoV-2 under the IDCRP
585 Epidemiology, Immunology, and Clinical Characteristics of Emerging Infectious Diseases with
586 Pandemic Potential (EPICC, IDCRP-085) protocol; a prospective, longitudinal study to analyze
587 COVID-19 disease. Subjects were enrolled at five hospitals across the continental U.S.,
588 including Walter Reed National Military Medical Center (WRNMMC, Bethesda, MD), Brooke
589 Army Medical Center (BAMC, San Antonio, TX), Naval Medical Center San Diego (NMCS,

590 San Diego, CA), Madigan Army Medical Center (MAMC, Tacoma, WA) and Fort Belvoir
591 Community Hospital (FBCH, Fort Belvoir, VA). Subjects of all race and gender seeking
592 treatment for acute illness at these military hospitals were offered enrollment into the EPICC,
593 IDCRP-085 protocol. Study enrollment included subjects with laboratory-confirmed SARS-CoV-
594 2 infection by nucleic acid amplification test, subjects with compatible illness in whom SARS-
595 CoV-2 infection is initially suspected but PCR confirmed as SARS-CoV-2 negative, and
596 asymptomatic subjects at risk of SARS-CoV-2 due to high risk exposure. In this study, 422
597 sera samples from 204 individual subjects were tested. The earliest serum samples collected \geq
598 10 dpso from subjects with longitudinal samples were included in positive performance
599 agreement. Additionally, serum samples from 35 subjects undergoing treatment at the COVID-
600 19 field hospital at the Jacob K. Javits Convention Center (New York, NY) under the COVID-19
601 Antibody Prevalence in Military Personnel Deployed to New York (COVID-19 NYC) protocol
602 were included in the assessment of assay performance. EPICC, IDCRP-085 and COVID-19
603 NYC protocols were approved by the Uniformed Services University Institutional Review Board.

604 *Multiplex microsphere-based immunoassay screening procedures*

605 Serum samples were collected from venipuncture in serum separator tubes, processed
606 and stored at -80°C in 250 μL aliquots until use. For each 96-well plate, a multiplex master mix
607 of antigen-coupled microspheres was made by diluting 100 μL of each antigen-coupled
608 microsphere working stock into 10 mL (1:100) 1XPBS without calcium and magnesium (Corning
609 Inc., Corning, NY) (all mentions of PBS refer to solutions without calcium and magnesium), and
610 100 μL of this master mix were added to each well so that each well contained 1 μL (~23 ng) of
611 each antigen-coupled microsphere per well. Wells were washed with 1XPBS + 0.05% Tween20
612 + 0.02% sodium azide two times. One hundred microliters of each serum sample was added to
613 each well. Serum samples were initially diluted within a class II type A2 biological safety cabinet
614 (BSC) then subjected to thermal inactivation for 30 min at 60°C , further serum dilutions are

615 noted in each respective figure legend. Human serum samples (1.25 μ L) were diluted 1:400 in
616 PBS and tested in technical duplicate A and B plates. Controls on each duplicate plate included
617 a PBS blank (wells: A1, B1, G12, H12) and positive (C1, F12) and negative (D1, E12) non-
618 human primate serum. As testing progressed, PCR and serology confirmed human
619 positive/negative samples replaced non-human primate serum samples as the qualified controls
620 for inter- and intra-plate variation.

621 Samples were incubated at room temperature for 45 minutes with agitation (900 rpm),
622 and plates were washed three times. Secondary antibody (goat anti-human IgG cross-absorbed
623 biotin-conjugated or goat anti-human IgM cross-absorbed biotin-conjugated; Thermo Fisher
624 Scientific, Waltham, MA) was diluted 1:5000 in 1XPBS + 0.05% Tween20 (PBST) and 100 μ L of
625 each secondary was added to each well and incubated for 45 minutes with agitation, and plates
626 were washed three times. Streptavidin-phycoerythrin (Bio-Rad) was diluted 1:1000 in PBST and
627 100 μ L was then added to each well and incubated for 30 minutes with agitation, and plates
628 were washed three times. Lastly, 100 μ L of PBST was added to each well and plates were
629 resuspended by agitation for 5 minutes. Plates were read on Bio-Plex 200 multiplexing systems
630 (Bio-Rad) with PMT voltage setting to the High RP1 target and 100 bead count requirements.
631 The MFI for the four PBS blank wells on each plate were subtracted from the MFI of each
632 sample well and MFI values for samples are reported as the PBS adjusted average from
633 duplicate plates.

634 *Threshold cutoffs for SARS-CoV-2 antibody*

635 To establish threshold cutoffs for SARS-CoV-2 spike protein-specific antibody reactivity,
636 we tested 127 archival acute and convalescent human serum samples from ARIC. Acute and
637 convalescent serum samples were collected within approximately three and twenty-eight days
638 of symptom onset, respectively. A cut-off of three times the mean MFI obtained using a mock
639 antigen preparation coupled microsphere was initially used to determine positivity of cross-

640 reactive antibodies in archival serum samples. As cross-reactive antibodies were found to occur
641 in 4 out of 45 serum samples from archival HCoV PCR-positive individuals, we then established
642 a cut-off of three standard deviations above the mean (99.7% probability) MFI of these archival
643 HCoV convalescent serum samples (n= 43) to establish a positivity threshold for detection of
644 SARS-CoV-2 spike protein reactive IgG and IgM antibodies. The remaining 84 archival serum
645 samples were tested against this MFI threshold cutoff for SARS-CoV-2 reactivity. The 127
646 archival ARIC serum samples were tested in technical duplicates in three independent
647 experiments to establish threshold cutoffs and specificity for SARS-CoV-2.

648 *Enzyme-linked immunosorbent assay*

649 Flat bottom 96-well microtiter plates (Corning) were coated with 300 ng of SARS-CoV-2
650 spike protein per well diluted in 100 μ l of ELISA coating buffer (1XPBS, 5.3g Na_2CO_3 , 4.2g
651 NaHCO_3 , pH 9.6) and incubated overnight at 4 $^\circ\text{C}$. The next day, spike protein was removed
652 and 125 μ l of 5% BSA blocking buffer were added to each well and incubated for 1 hour at 37
653 $^\circ\text{C}$. SARS-CoV-2 spike protein coated and blocked plates were then washed three times
654 with 200 μ l PBST. Serum samples were subjected to thermal inactivation after being initially
655 diluted in a BSC. Inactivated serum samples were then serially diluted 2-fold in PBS. One
656 hundred microliters of each dilution was added in duplicate to the antigen coated plate, sealed,
657 and incubated at 37 $^\circ\text{C}$ for 1 hour. Plates were then washed three times with 200 μ l PBST. One
658 hundred microliters of secondary antibody, anti-human (H&L) HRP conjugated, diluted 1:5000 in
659 PBS to each well was added to each well and plates were incubated at 37 $^\circ\text{C}$ for 1 hour. Plates
660 were then washed three times with 200 μ l PBST. Eighty-five microliters ABST Substrate
661 Solution (Thermo Fisher Scientific) was added to each well and plates were agitated (900 rpm)
662 at room temperature for 30 minutes, then analyzed at 650 nm absorbance on a plate reader
663 (Molecular Devices, San Jose, CA).

664 *Statistical analysis*

665 Figures were generated and statistical analyses were performed in GraphPad Prism
666 version 7.0. The positive predictive value and negative predictive value were calculated with
667 MedCalc statistical software. ROC analysis was conducted using R version 4.0.2.

668

669 **REFERENCES**

670

- 671 1. E. Petersen *et al.*, Comparing SARS-CoV-2 with SARS-CoV and influenza pandemics.
672 *Lancet Infect Dis* **20**, e238-e244 (2020).
- 673 2. A. Wu *et al.*, Genome Composition and Divergence of the Novel Coronavirus (2019-
674 nCoV) Originating in China. *Cell Host Microbe* **27**, 325-328 (2020).
- 675 3. F. J. Ibarondo *et al.*, Rapid Decay of Anti-SARS-CoV-2 Antibodies in Persons with Mild
676 Covid-19. *N Engl J Med* 10.1056/NEJMc2025179 (2020).
- 677 4. Q. X. Long *et al.*, Clinical and immunological assessment of asymptomatic SARS-CoV-2
678 infections. *Nat Med* **26**, 1200-1204 (2020).
- 679 5. J. Seow *et al.*, Longitudinal evaluation and decline of antibody responses in SARS-CoV-
680 2 infection. *medRxiv* 10.1101/2020.07.09.20148429, 2020.2007.2009.20148429 (2020).
- 681 6. E. Hartenian *et al.*, The molecular virology of Coronaviruses. *J Biol Chem*
682 10.1074/jbc.REV120.013930 (2020).
- 683 7. U.S. Food and Drug Administration (2020, September 11) EUA authorized serology test
684 performance. [https://www.fda.gov/medical-devices/coronavirus-disease-2019-covid-19-](https://www.fda.gov/medical-devices/coronavirus-disease-2019-covid-19-emergency-use-authorizations-medical-devices/eua-authorized-serology-test-performance)
685 [emergency-use-authorizations-medical-devices/eua-authorized-serology-test-](https://www.fda.gov/medical-devices/coronavirus-disease-2019-covid-19-emergency-use-authorizations-medical-devices/eua-authorized-serology-test-performance)
686 [performance](https://www.fda.gov/medical-devices/coronavirus-disease-2019-covid-19-emergency-use-authorizations-medical-devices/eua-authorized-serology-test-performance)

- 687 8. A. Ayouba *et al.*, Development of a Sensitive and Specific Serological Assay Based on
688 Luminex Technology for Detection of Antibodies to Zaire Ebola Virus. *J Clin Microbiol*
689 **55**, 165-176 (2017).
- 690 9. R. L. Powell *et al.*, A Multiplex Microsphere-Based Immunoassay Increases the
691 Sensitivity of SIV-Specific Antibody Detection in Serum Samples and Mucosal
692 Specimens Collected from Rhesus Macaques Infected with SIVmac239. *Biores Open*
693 *Access* **2**, 171-178 (2013).
- 694 10. N. G. Satterly, M. A. Voorhees, A. D. Ames, R. J. Schoepp, Comparison of MagPix
695 Assays and Enzyme-Linked Immunosorbent Assay for Detection of Hemorrhagic Fever
696 Viruses. *J Clin Microbiol* **55**, 68-78 (2017).
- 697 11. R. Kozak *et al.*, Severity of coronavirus respiratory tract infections in adults admitted to
698 acute care in Toronto, Ontario. *J Clin Virol* **126**, 104338 (2020).
- 699 12. S. Nickbakhsh *et al.*, Extensive multiplex PCR diagnostics reveal new insights into the
700 epidemiology of viral respiratory infections. *Epidemiol Infect* **144**, 2064-2076 (2016).
- 701 13. S. Su *et al.*, Epidemiology, Genetic Recombination, and Pathogenesis of Coronaviruses.
702 *Trends Microbiol* **24**, 490-502 (2016).
- 703 14. B. Freeman *et al.*, Validation of a SARS-CoV-2 spike protein ELISA for use in contact
704 investigations and serosurveillance. *bioRxiv : the preprint server for biology*
705 10.1101/2020.04.24.057323, 2020.2004.2024.057323 (2020).
- 706 15. J. Hicks *et al.*, Serologic cross-reactivity of SARS-CoV-2 with endemic and seasonal
707 Betacoronaviruses. *medRxiv* 10.1101/2020.06.22.20137695 (2020).
- 708 16. V. J. Munster *et al.*, Respiratory disease in rhesus macaques inoculated with SARS-
709 CoV-2. *Nature* 10.1038/s41586-020-2324-7 (2020).
- 710 17. W. Deng *et al.*, Primary exposure to SARS-CoV-2 protects against reinfection in rhesus
711 macaques. *Science* **369**, 818-823 (2020).

- 712 18. S. Lu *et al.*, Comparison of nonhuman primates identified the suitable model for COVID-
713 19. *Signal Transduct Target Ther* **5**, 157 (2020).
- 714 19. C. Shan *et al.*, Infection with novel coronavirus (SARS-CoV-2) causes pneumonia in
715 Rhesus macaques. *Cell Res* **30**, 670-677 (2020).
- 716 20. M. Norman *et al.*, Ultrasensitive high-resolution profiling of early seroconversion in
717 patients with COVID-19. *Nature Biomedical Engineering* 10.1038/s41551-020-00611-x
718 (2020).
- 719 21. L. Liu *et al.*, A preliminary study on serological assay for severe acute respiratory
720 syndrome coronavirus 2 (SARS-CoV-2) in 238 admitted hospital patients. *Microbes and*
721 *infection* **22**, 206-211 (2020).
- 722 22. B. Lou *et al.*, Serology characteristics of SARS-CoV-2 infection after exposure and post-
723 symptom onset. *European Respiratory Journal* **56**, 2000763 (2020).
- 724 23. L. Guo *et al.*, Profiling Early Humoral Response to Diagnose Novel Coronavirus Disease
725 (COVID-19). *Clinical Infectious Diseases* **71**, 778-785 (2020).
- 726 24. N. M. A. Okba *et al.*, Severe Acute Respiratory Syndrome Coronavirus 2–Specific
727 Antibody Responses in Coronavirus Disease Patients. *Emerging Infectious Disease*
728 *journal* **26**, 1478 (2020).
- 729 25. L. Premkumar *et al.*, The receptor-binding domain of the viral spike protein is an
730 immunodominant and highly specific target of antibodies in SARS-CoV-2 patients.
731 *Science Immunology* **5**, eabc8413 (2020).
- 732 26. F. Amanat *et al.*, A serological assay to detect SARS-CoV-2 seroconversion in humans.
733 *Nat Med* **26**, 1033-1036 (2020).
- 734 27. C. Klumpp-Thomas *et al.*, Standardization of enzyme-linked immunosorbent assays for
735 serosurveys of the SARS-CoV-2 pandemic using clinical and at-home blood sampling.
736 *medRxiv* 10.1101/2020.05.21.20109280 (2020).

- 737 28. F. Wu *et al.*, Neutralizing antibody responses to SARS-CoV-2 in a COVID-19 recovered
738 patient cohort and their implications. *medRxiv* 10.1101/2020.03.30.20047365,
739 2020.2003.2030.20047365 (2020).
- 740 29. C. W. Tan *et al.*, A SARS-CoV-2 surrogate virus neutralization test based on antibody-
741 mediated blockage of ACE2-spike protein-protein interaction. *Nat Biotechnol* **38**, 1073-
742 1078 (2020).
- 743 30. L. Liu *et al.*, Potent neutralizing antibodies against multiple epitopes on SARS-CoV-2
744 spike. *Nature* **584**, 450-456 (2020).
- 745 31. C. O. Barnes *et al.*, Structures of Human Antibodies Bound to SARS-CoV-2 Spike
746 Reveal Common Epitopes and Recurrent Features of Antibodies. *Cell* **182**, 828-
747 842.e816 (2020).
- 748 32. X. Chi *et al.*, A neutralizing human antibody binds to the N-terminal domain of the Spike
749 protein of SARS-CoV-2. *Science* **369**, 650-655 (2020).
- 750 33. D. F. Robbiani *et al.*, Convergent antibody responses to SARS-CoV-2 in convalescent
751 individuals. *Nature* **584**, 437-442 (2020).
- 752 34. P. J. M. Brouwer *et al.*, Potent neutralizing antibodies from COVID-19 patients define
753 multiple targets of vulnerability. *Science* **369**, 643-650 (2020).
- 754 35. D. Pinto *et al.*, Cross-neutralization of SARS-CoV-2 by a human monoclonal SARS-CoV
755 antibody. *Nature* **583**, 290-295 (2020).
- 756 36. L. Wang *et al.*, Importance of Neutralizing Monoclonal Antibodies Targeting Multiple
757 Antigenic Sites on the Middle East Respiratory Syndrome Coronavirus Spike
758 Glycoprotein To Avoid Neutralization Escape. *Journal of Virology* **92**, e02002-02017
759 (2018).
- 760 37. L. M. Mayr, B. Su, C. Moog, Non-Neutralizing Antibodies Directed against HIV and Their
761 Functions. *Frontiers in immunology* **8**, 1590-1590 (2017).

- 762 38. E. O. Saphire, S. L. Schendel, B. M. Gunn, J. C. Milligan, G. Alter, Antibody-mediated
763 protection against Ebola virus. *Nat Immunol* **19**, 1169-1178 (2018).
- 764 39. S. J. Zost *et al.*, Potently neutralizing and protective human antibodies against SARS-
765 CoV-2. *Nature* **584**, 443-449 (2020).
- 766 40. J. Zang *et al.*, Immunization with the receptor-binding domain of SARS-CoV-2 elicits
767 antibodies cross-neutralizing SARS-CoV-2 and SARS-CoV without antibody-dependent
768 enhancement. *Cell Discov* **6**, 61-61 (2020).
- 769 41. D. F. Gudbjartsson *et al.*, Spread of SARS-CoV-2 in the Icelandic Population. *N Engl J*
770 *Med* **382**, 2302-2315 (2020).
- 771 42. D. Esposito *et al.*, Optimizing high-yield production of SARS-CoV-2 soluble spike trimers
772 for serology assays. *bioRxiv* 10.1101/2020.05.27.120204 (2020).
- 773 43. R. N. Kirchdoerfer *et al.*, Stabilized coronavirus spikes are resistant to conformational
774 changes induced by receptor recognition or proteolysis. *Sci Rep* **8**, 15701 (2018).
- 775 44. D. Wrapp *et al.*, Cryo-EM structure of the 2019-nCoV spike in the prefusion
776 conformation. *Science* **367**, 1260-1263 (2020).
- 777 45. C. Coles, E. V. Millar, T. Burgess, M. G. Ottolini, The Acute Respiratory Infection
778 Consortium: A Multi-Site, Multi-Disciplinary Clinical Research Network in the Department
779 of Defense. *Mil Med* **184**, 44-50 (2019).
- 780 46. M. Bouvier *et al.*, Species-specific clinical characteristics of human coronavirus infection
781 among otherwise healthy adolescents and adults. *Influenza Other Respir Viruses* **12**,
782 299-303 (2018).

783
784

785

786

787

788 **TABLES**

789 **Table 1. MMIA SARS-CoV-2 spike protein performance**

	SARS-CoV-2 PCR Status/Archival Sera			
		Positive ¹	Negative	Total
SARS-CoV-2 MMIA IgG Antibody Test ²	Positive	152	0	152
	Negative	3	117	120
	Total	155	117	272
	Sensitivity	98.1%		
	Specificity	100%		
SARS-CoV-2 MMIA IgM Antibody Test ³	Positive	82	0	82
	Negative	23	117	140
	Total	105	117	222
	Sensitivity	78.1%		
	Specificity	100%		

790 ¹84 archival serum samples and 33 serum samples from PCR negative study enrollees are
791 included as SARS-CoV-2 negative.

792 ²IgG antibody test included serum samples from n= 155 PCR positive subjects including 82
793 EPICC outpatients, 38 EPICC hospitalized subjects and 35 COVID-19 NYC hospitalized
794 subjects

795 ³IgM antibody test included serum samples from n= 105 PCR positive subjects including 41
796 EPICC outpatients, 29 EPICC hospitalized subjects and 35 COVID-19 NYC hospitalized
797 subjects

798

799
800

801 **Table 2. MMIA SARS-CoV-2 RBD performance**

	SARS-CoV-2 PCR Status/Archival Sera			
		Positive	Negative	Total
SARS-CoV-2 MMIA IgG Antibody Test	Positive	135	0	135
	Negative	20	117	137
	Total	155	117	266
	Sensitivity	87.1%		
	Specificity	100%		

802

803 **Table 3. IgG and IgM seropositivity within 28 days post-symptom onset (dpso)**

dpso	IgG+	IgG+/IgM+
7 – 14	80.0% (12/15)	73.3% (11/15)
15 – 28	100% (31/31)	93.5% (29/31)

804

805

806

807

808

809

810

811

812

813

814

815

816 **DECLARATIONS**

817 These research protocols, IDCRP-085, IDCRP-045 and COVID-19 NYC, were approved by the
818 USU IRB.

819

820 **CONFLICT OF INTEREST**

821 None of the authors have any conflicts of interest of relevance to disclose.

822

823 **DISCLAIMER**

824 The contents of this publication are the sole responsibility of the author(s) and do
825 not necessarily reflect the views, opinions, or policies of the Uniformed Services University
826 (USU), the Henry M. Jackson Foundation for the Advancement of Military Medicine, Inc. (HJF),
827 National Institutes of Health or the Department of Health and Human Services, Brooke Army
828 Medical Center, the U.S. Army Medical Department, the U.S. Army Office of the Surgeon
829 General, the US Department of Defense (DoD), the Departments of the Air Force, Army or
830 Navy, or the U.S. Government. Mention of trade names, commercial products, or organization
831 does not imply endorsement by the U.S. Government. A number of the co-authors are military
832 service members (or employees of the U.S. Government). This work was prepared as part of
833 their official duties. Title 17 U.S.C. §105 provides that 'Copyright protection under this title is not
834 available for any work of the United States Government.' Title 17 U.S.C. §101 defines a U.S.
835 Government work as a work prepared by a military service member or employee of the U.S.
836 Government as part of that person's official duties.

837

838 **FUNDING**

839 This project has been funded by the National Institute of Allergy and Infectious Diseases,
840 National Institutes of Health, under Inter-Agency Agreement Y1-AI-5072 and the Defense
841 Health Program, U.S. DoD, under award HU0001190002. This project has been funded in part

842 with Federal funds from the National Cancer Institute, National Institutes of Health, under
843 contract number HHSN261200800001E. VJM and EdW are supported by the Intramural
844 Research Program of the National Institutes of Allergy and Infectious Diseases.

845

846 **ACKNOWLEDGEMENTS**

847 We thank Kelly Snead, Vanessa Wall, John-Paul Denson, Simon Messing, and William
848 Gillette (Protein Expression Lab, FNCLR) for excellent technical assistance. We also
849 thank Scott Merritt and Katrin Mende (IDCRP, HJF, Brooke Army Medical Center) and
850 Kathleen Pratt (Department of Medicine, USUHS) for assistance with sample
851 acquisition.

852

853

854